2080 *Organometallics* **2003,** *22,* 2080−2086

Molecular Structure and Vinyl Chloride Insertion of a Cationic Zirconium(IV) Acyl Carbonyl Complex

Han Shen and Richard F. Jordan*

Department of Chemistry, The University of Chicago, 5735 South Ellis Avenue,
Chicago, Illinois 60637

Received December 20, 2002

The reaction of vinyl chloride (VC) with the cationic Zr acyl complex $[Cp_2Zr\{C(=O)Me\}(CO)][MeB(C_6F_5)_3]$ (**1a**/**b**, O-inside and O-outside isomers) yields an unusual dinuclear dicationic μ-acyl μ-keto-alkoxide complex, $[Cp_2Zr\{\mu\text{-}C(=O)Me\}\{\mu\text{-}OCMe(CH=CH_2)C(=O)Me\}ZrCp_2][MeB(C_6F_5)_3]_2$ (**3**), which was characterized by NMR spectroscopy and X-ray crystallography. This reaction proceeds by 1,2 insertion into the Zr−acyl bond of $Cp_2Zr\{C(=O)Me\}^+$ to yield $Cp_2Zr\{CH_2CHClC(=O)Me\}^+$, which undergoes β-Cl elimination to form methyl vinyl ketone (MVK) and Cp_2ZrCl^+ (**8**). The MVK is trapped by $Cp_2Zr\{C(=O)Me\}^+$ to form $[Cp_2Zr\{\eta^2\text{-}C(=O)Me\}(MVK)][MeB(C_6F_5)_3]$ (**9**), which rearranges to $[Cp_2Zr\{\kappa^2\text{-}OC(Me)(CH=CH_2)C(=O)Me\}][MeB(C_6F_5)_3]$ (**10**). Intermediate **10** is trapped by $Cp_2Zr\{C(=O)Me\}^+$ to form **3**. **3** is also formed by the reaction of **1a**/**b** with 0.5 equiv of MVK. 1,2 VC insertion of $Cp_2Zr\{C(=O)Me\}^+$ is favored over 2,1 insertion by steric factors. The molecular structure of **1a** was determined by X-ray crystallography.

Introduction

The synthesis of new materials by insertion polymerization/copolymerization of vinyl chloride (VC) using metal catalysts is an attractive goal because this approach may enable better control of polymer structure and properties than is possible by conventional radical methods.[1] We showed previously that $(C_5R_5)_2ZrR^+$, $(C_5Me_4SiMe_2N^tBu)TiR^+$, $(Me_2bipy)PdR^+$, $\{ArN=C(Me)C(Me)=NAr\}PdMe^+$ ($Ar = 2,6\text{-}^iPr_2\text{-}C_6H_3$), and (salicylaldiminato)Ni(Ph)(PPh$_3$) complexes readily insert VC to yield $L_nMCH_2CHClR^+$ intermediates, which undergo β-Cl elimination to produce M−Cl species and the corresponding $CH_2=CHR$ olefin.[2] The β-Cl elimination reaction precludes homopolymerization of VC or copolymerization of VC with other olefins by these catalysts. Analogous 1,2 insertion/β-X elimination reactions of $CH_2=CHX$ substrates with $(^tBu_3SiO)_3TaH_2$, Cp_2ZrHCl, $\{2,6\text{-}(o\text{-tol-}N=CMe)_2pyridine\}FeCl_2$/MAO, and $\{ArN=C(Me)C(Me)=NAr\}PdMe^+$ have also been reported.[3]

In an effort to circumvent β-Cl elimination, we investigated the reactions of $L_2Pd\{C(=O)Me\}^+$ acyl complexes with VC. These reactions proceed by 2,1 VC insertion to yield O-chelated $L_2Pd\{CHClCH_2C(=O)Me\}^+$ products which cannot β-Cl eliminate because they do not have a β-Cl substituent.[4] However, the chelated species do not react further with CO, VC, or ethylene due to the robustness of the chelate rings and the low migratory aptitude of the α-Cl-substituted $-CHClCH_2C(=O)Me$ group. We hypothesized that analogous but more reactive $L_nM\{CHClCH_2C(=O)R\}^+$ species might form by 2,1 VC insertion into other $L_nM\{C(=O)R\}^+$ catalysts. To study this possibility, we investigated the reaction of VC with $Cp_2Zr\{\eta^2\text{-}C(=O)Me\}^+$, which is known to insert alkynes and alkenes.[5−7] In fact, we have found that this species undergoes 1,2 VC insertion, which ultimately leads to an unusual dinuclear product. During the course of this work we also determined the molecular structure of the Zr(IV) carbonyl complex $[Cp_2Zr\{\eta^2\text{-}C(=O)Me\}(CO)][MeB(C_6F_5)_3]$ (O-inside isomer).

Results and Discussion

Generation of $[Cp_2Zr\{\eta^2\text{-}C(=O)Me\}(CO)][MeB(C_6F_5)_3]$ (1a/b). We showed previously that the Zr(IV) acyl carbonyl complex $[Cp_2Zr\{\eta^2\text{-}C(=O)Me\}(CO)][MeB(C_6F_5)_3]$ is generated as a mixture of “O-inside” and “O-outside” isomers (**1a**/**1b** = 5:1 at 23 °C) in quantitative yield by the reaction of $Cp_2ZrMe(\mu\text{-}Me)B(C_6F_5)_3$ with CO (3 atm) in CD_2Cl_2 (eq 1).[6] The analogous $Cp^*{}_2Zr\{\eta^2\text{-}C(=O)Me\}(CO)^+$ cation ($Cp^* = C_5Me_5$) is generated in a

---

[1] (a) Vinyl Chloride and Poly (Vinyl Chloride). *Kirk-Othmer Encyclopedia of Chemical Technology*, 3rd ed.; Wiley & Sons: New York, 1983; Vol. 23, pp 865−936. (b) Kirk-Othmer Encyclopedia of Chemical Technology Home Page. http://www.mrw.interscience.wiley.com/kirk/ (accessed July 2002).

[2] (a) Stockland, R. A., Jr.; Jordan, R. F. *J. Am. Chem. Soc.* **2000**, *122*, 6315. (b) Jordan, R. F.; Stockland, R. A., Jr.; Shen, H.; Foley, S. *Polym. Mater. Sci. Eng.* **2002**, *87*, 39. (c) Jordan, R. F. *Polym. Prepr.* (*Am. Chem. Soc., Div. Polym. Chem.*) **2001**, *42*, 829. (d) Stockland, R. A., Jr.; Foley, S. R.; Jordan, R. F. *J. Am. Chem. Soc.* **2003**, *125*, 796. (e) Foley, S. R.; Stockland, R. A., Jr.; Shen, H.; Jordan, R. F. *J. Am. Chem. Soc.* **2003**, ASAP.

[3] (a) Strazisar, S. A.; Wolczanski, P. T. *J. Am. Chem. Soc.* **2001**, *123*, 4728. (b) Watson, L. A.; Yandulov, D. V.; Caulton, K. G. *J. Am. Chem. Soc.*, **2001**, *123*, 603. (c) Boone, H.; Athey, P. S.; Mullins, M. J.; Philipp, D.; Muller, R.; Goddard, W. A. *J. Am. Chem. Soc.* **2002**, *124*, 8790. (d) Kang, M.; Sen, A.; Zakharov, L.; Rheingold, A. L. *J. Am. Chem. Soc.* **2002**, *124*, 12080.

[4] L_2 = 4,4′-Me$_2$-2,2′-bipyridine (Me$_2$bipy), 4,4′-^{t}Bu$_2$-2,2′-bipyridine (^{t}Bu$_2$bipy), 1,3-bis(diphenylphosphino)propane (dppp), 1,2-bis(dimethylphosphino)ethane (dmpe)). Shen, H.; Jordan, R. F. *Organometallics* **2003**, in press.

[5] Shen, H.; Jordan, R. F. *Abstr. Pap. Am. Chem. Soc.* **2002**, *224*, 640-INOR.

[6] (a) Guo, Z.; Swenson, D. C.; Guram, A. S.; Jordan, R. F. *Organometallics* **1994**, *13*, 766. (b) Guram, A. S.; Guo, Z.; Jordan, R. F. *J. Am. Chem. Soc.* **1993**, *115*, 4902.

[7] Busico, V.; Guardasole, M.; Margonelli, A.; Segre, A. L. *J. Am. Chem. Soc.* **2000**, *122*, 5226.

10.1021/om0210311 CCC: $25.00
Publication on Web 03/27/2003

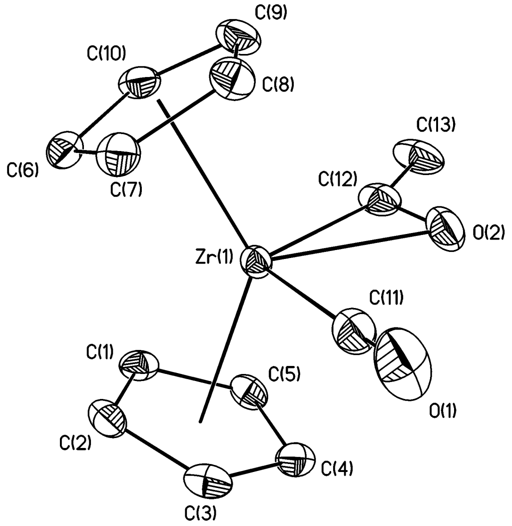

Figure 1. ORTEP view of the cation of **1a**. Hydrogen atoms are omitted.

similar fashion and favors the "O-outside" form (**2a**/**2b** = 1:9); **2b** was characterized by X-ray diffraction. These species are rare examples of d^0 metal carbonyl complexes.[8] The ν_{CO} values for the O-inside isomers **1a** (2176 cm^{-1}) and **2a** (2152 cm^{-1}) are higher than the free CO value (2143 cm^{-1}), reflecting the absence of d$-\pi^*$ back-bonding. However the ν_{CO} values for the O-outside isomers **1b** (2123 cm^{-1}) and **2b** (2105 cm^{-1}) are slightly lower than the free CO value, due to nonclassical back-bonding from a filled Zr-acyl σ orbital to a CO π^* orbital.[6] Complex **1a**/**b** undergoes irreversible loss of CO if the CO pressure is reduced to ca. 1 atm, leading to the precipitation of the insoluble compound $Cp_2Zr\{\eta^2\text{-}C({=}O)Me\}(\mu\text{-}Me)B(C_6F_5)_3$.

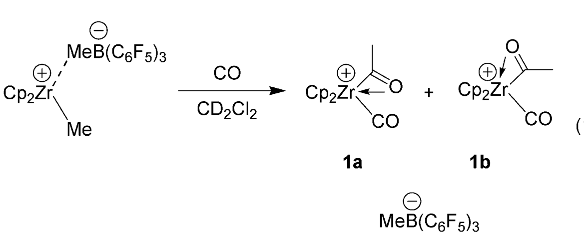

(1)

X-ray Structure of 1a. Isomer **1a** selectively crystallizes from a CH_2Cl_2 solution of **1a**/**b** at −80 °C and was characterized by X-ray diffraction. The solid state structure of **1a** consists of discrete $Cp_2Zr\{\eta^2\text{-}C({=}O)Me\}(CO)^+$ and $MeB(C_6F_5)_3^-$ ions. The closest cation−anion contact is between a Cp hydrogen and a meta-fluorine (H(3)- - -F(2) = 2.491 Å) and is somewhat shorter than the sum of the van der Waals radii (ca. 2.67 Å).[9] An ORTEP view of the $Cp_2Zr\{\eta^2\text{-}C({=}O)Me\}(CO)^+$ cation of **1a** is shown in Figure 1, and selected bond distances and bond angles are given in Table 1.

The $Cp_2Zr\{\eta^2\text{-}C({=}O)Me\}(CO)^+$ cation adopts a bent metallocene structure with centroid−Zr−centroid angles and Zr−centroid distances in the range observed for other Cp_2Zr complexes.[10,11] The η^2-acyl and CO ligands are located in the plane between the two Cp ligands, and the Zr(1), O(1), O(2), C(11), C(12), and C(13) atoms are essentially coplanar. The η^2-acyl group is structurally similar to that in **2b**. The Zr−O distance and Zr−C−O angle in **1a** (Zr(1)−O(2) 2.251(3) Å, Zr(1)−C(12)−O(2) = 76.8(3)°) are nearly identical to the corresponding values in **2b** (2.242(7) Å, 74.7(6)°), but the Zr−C distance in **1a** (Zr(1)−C(12) = 2.184(4) Å) is slightly shorter than that in **2b** (2.22(1) Å). The $Zr-C_{acyl}$ and Zr−O distances in **1a** are slightly shorter than the corresponding distances in the neutral analogue $Cp_2Zr\{C({=}O)Me\}Me$ (O-inside isomer; $Zr-C_{acyl}$ = 2.197(6) Å, Zr−O = 2.290(4) Å), consistent with the highly electrophilic character of the cationic Zr(IV) center.[12] Interestingly, the Zr−CO bond (Zr(1)−C(11) = 2.366(4) Å) in **1a** is ca. 0.11 Å longer than that in **2b** (2.25(1) Å). This difference and the difference in $Zr-C_{acyl}$ distances noted above reflect the presence of $\sigma_{Zr-C(acyl)}-\pi^*_{CO}$ back-bonding in the latter species. The Zr−CO distances in **1a** and **2b** are far longer than those in Zr(II) carbonyl complexes, e.g., $Cp_2Zr(CO)_2$ (2.187(4) Å),[13] $Cp^*_2Zr(CO)_2$ (2.145(9) Å),[14] which possess strong d$-\pi^*$ back-bonding. These structural results support the bonding analysis for $(C_5R_5)_2Zr\{C({=}O)Me\}(CO)^+$ species developed previously based on IR and computational results.[6]

Table 1. Selected Bond Lengths (Å) and Angles (deg) for 1a

Zr(1)−C(11)	2.366(4)	Zr(1)−C(12)	2.184(4)
Zr(1)−O(2)	2.251(3)	C(12)−C(13)	1.490(6)
C(12)−O(2)	1.240(5)	C(11)−O(1)	1.117(5)
Zr(1)−C100[a]	2.184	Zr(1)−C200[a]	2.190
C(11)−Zr(1)−C100	97.7	C(11)−Zr(1)−C200	98.9
C(12)−Zr(1)−C100	111.2	C(12)−Zr(1)−C200	106.0
O(2)−Zr(1)−C100	116.2	O(2)−Zr(1)−C200	113.7
C100−Zr(1)−C200	133.4	Zr(1)−C(11)−O(1)	175.6(4)
Zr(1)−C(12)−O(2)	76.8(3)	Zr(1)−C(12)−C(13)	159.7(3)
O(2)−C(12)−C(13)	123.6(4)	O(2)−Zr(1)−C(12)	32.4(1)
C(11)−Zr(1)−C(12)	111.9(2)	C(11)−Zr(1)−O(2)	79.5(1)

[a] C100 is the centroid of the C(1)−C(5) Cp ring; C200 is the centroid of the C(6)−C(10) Cp ring.

Reaction of VC with $Cp_2Zr\{\eta^2\text{-}C({=}O)Me\}^+$. The reaction of **1a**/**b** with VC was performed by freezing a CD_2Cl_2 solution of **1a**/**b** at −196 °C, removing the gaseous CO under vacuum, adding VC (ca. 14 equiv) at

---

(8) Lupinetti, A. J.; Strauss, S. H.; Frenking, G. *Prog. Inorg. Chem.* **2001**, *49*, 1.

(9) van der Waals radii (H: 1.20 Å; F: 1.47 Å) taken from Bondi, A. *J. Phys. Chem.* **1964**, *68*, 441.

(10) (a) Ryan, E. J. Bis(cyclopentadienyl)zirconium and -hafnium Halide Complexes in Oxidation State +4. In *Comprehensive Organometallic Chemistry II*: *A Review of the Literature 1982−1994*; Abel, E. W., Stone, F. G. A., Wilkinson, G., Lappert, M. F., Eds.; Elsevier Science Inc.: New York, 1995; Vol. 4, pp 483−499. (b) Cardin, D. J.; Lappert, M. F.; Raston, C. L. *Chemistry of Organo-Zirconium and -Hafnium Compounds*; Ellis Horwood: Chichester, 1986.

(11) (a) Guzei, I. A.; Stockland, R. A., Jr.; Jordan, R. F. *Acta Crystallogr.* **2000**, *C56*, 635. (b) Liu, F.-C.; Liu, J.; Meyers, E. A.; Shore, S. G. *Inorg. Chem.* **1999**, *38*, 2169. (c) Clegg, W.; Horsburgh, L.; Lindsay, D. M.; Mulvey, R. E. *Acta Crystallogr.* **1998**, *C54*, 315 (d) Lappert, M. F.; Raston, C. L.; Skelton, B. W.; White, A. H. *J. Chem. Soc., Dalton Trans.* **1997**, 2895. (e) Erker, G.; Frömberg, W.; Benn, R.; Mynott, R.; Angermund, K.; Krüger *Organometallics* **1989**, *8*, 911. (f) Bailey, S. I.; Colgan, D.; Engelhardt, L. M.; Leung, W.-P.; Papasergio, R. I.; Raston, C. L.; White, A. H. *J. Chem. Soc., Dalton Trans.* **1986**, 603. (g) Erker, G.; Czisch, P.; Mynott, R.; Tsay, Y.-H.; Krüger, C. *Organometallics* **1985**, *4*, 1310. (h) Hunter, W. E.; Hrncir, D. C.; Bynum, R. V.; Penttila, R. A.; Atwood, J. L. *Organometallics* **1983**, *2*, 750. (i) Atwood, J. L.; Barker, G. K.; Holton, J.; Hunter, W. E.; Lappert, M. F.; Pearce, R. *J. Am. Chem. Soc.* **1977**, *99*, 6645.

(12) Guram, A. S.; Jordan, R. F. Cationic Organozirconium and Organohafnium Complexes. In *Comprehensive Organometallic Chemistry II*: *A Review of the Literature 1982−1994*; Abel, E. W., Stone, F. G. A., Wilkinson, G., Lappert, M. F., Eds.; Elsevier Science Inc.: New York, 1995; Vol. 4, pp 589−625.

(13) Atwood, J. L.; Rogers, R. D.; Hunter, W. E.; Floriani, C.; Fachinetti, G.; Chiesi-Villa, A. *Inorg. Chem.* **1980**, *19*, 3812.

(14) Sikora, D. J.; Rausch, M. D.; Rogers, R. D.; Atwood, J. L. *J. Am. Chem. Soc.* **1981**, *103*, 1265.

−196 °C, and warming to 23 °C. Under these conditions a yellow crystalline solid starts to form within 1 h, and the reaction is complete after 12 h (eq 2). NMR analysis of the solid in THF-d_8 shows that it is a mixture of a dinuclear dicationic complex $[Cp_2Zr\{\mu\text{-}C({=}O)Me\}\{\mu\text{-}OCMe(CH{=}CH_2)C({=}O)Me\}ZrCp_2][MeB(C_6F_5)_3]_2$ (**3**, 79% vs **1a**/**b**), formed by reaction of **1a**/**b** with VC, and $Cp_2Zr\{\eta^2\text{-}C({=}O)Me\}(\mu\text{-}Me)B(C_6F_5)_3$ (2% vs **1a**/**b**), formed by loss of CO from **1a**/**b** and precipitation as described above.[15] The structure of **3** was established by X-ray diffraction, ^1H NMR spectroscopy, and alternate synthesis (vide infra). NMR analysis of the filtrate shows that Cp_2ZrCl_2, other unidentified Cp_2Zr species, and $B(C_6F_5)_3$ are present.

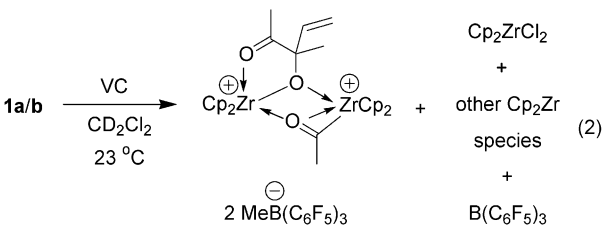

3

Alternate Synthesis of 3. The reaction of **1a**/**b** with 0.5 equiv of methyl vinyl ketone (MVK) in CD_2Cl_2 at 23 °C also affords **3** as a yellow crystalline solid in high yield (91%, eq 3). In contrast to the **3** produced in eq 2, the product of eq 3 is not contaminated by $Cp_2Zr\{\eta^2\text{-}C({=}O)Me\}(\mu\text{-}Me)B(C_6F_5)_3$.

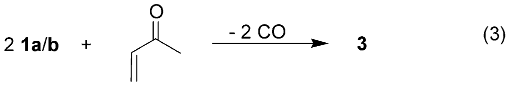

Molecular Structure of 3. Single crystals of **3** were isolated from the reactions of **1a**/**b** with VC (eq 2) and with MVK (eq 3) and were analyzed by X-ray diffraction. The two analyses are essentially identical, and only the latter is described here. **3** crystallizes as discrete cations and anions; there are no close cation−anion contacts. ORTEP views of the dinuclear dication of **3** are shown in Figure 2, and corresponding space-filling diagrams are shown in Figure 3. Selected bond distances and bond angles are listed in Table 2.

The dinuclear dication of **3** can be viewed as an adduct of two fragments: the η^2-acyl cation $Cp_2Zr\{\eta^2\text{-}C({=}O)Me\}^+$ and the O-chelated keto-alkoxide cation $Cp_2Zr\{\kappa^2\text{-}OCMe(CH{=}CH_2)C({=}O)Me\}^+$, which are bridged through O(1) and O(2). The ring formed by Zr(1), O(1), Zr(2), and O(2) is slightly puckered as O(2) deviates from the Zr(1)−Zr(2)−O(1) plane by 0.121 Å. Space-filling diagrams (Figure 3) show that the two fragments fit together snugly, which may explain why the formation of **3** is favored.

The structure of the $Cp_2Zr\{\eta^2\text{-}C({=}O)Me\}^+$ unit in **3** is very similar to that in **1a** except that the Zr(2)−O(1) distance (2.290(3) Å) is ca. 0.04 Å longer than the corresponding distance in **1a**, due to coordination of the second Zr center (Zr(1)) to the acyl oxygen. In fact, the Zr(1)−O(1) distance (2.181(3) Å) is in the range observed for Zr(IV) ketone complexes such as $Cl_4Zr\{O{=}C(Me)^tBu\}_2$ (2.192(2) Å)[16] and $[C_5Me_4\{CH_2B(C_6F_5)_3\}]Cp^*Zr(Ph)(O{=}CMe_2)$ (2.132(5) Å).[17] The keto-alkoxide ligand binds to

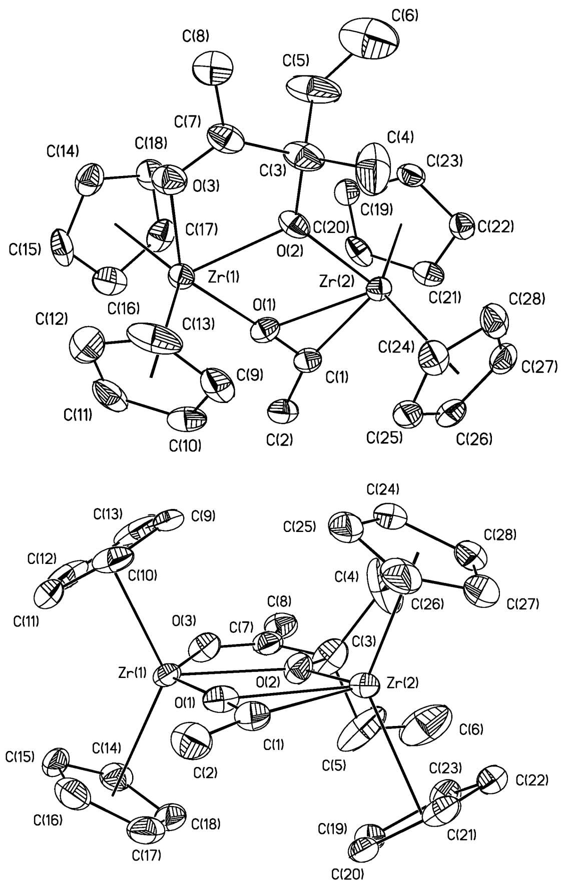

Figure 2. ORTEP views of the dication of **3**. Hydrogen atoms are omitted.

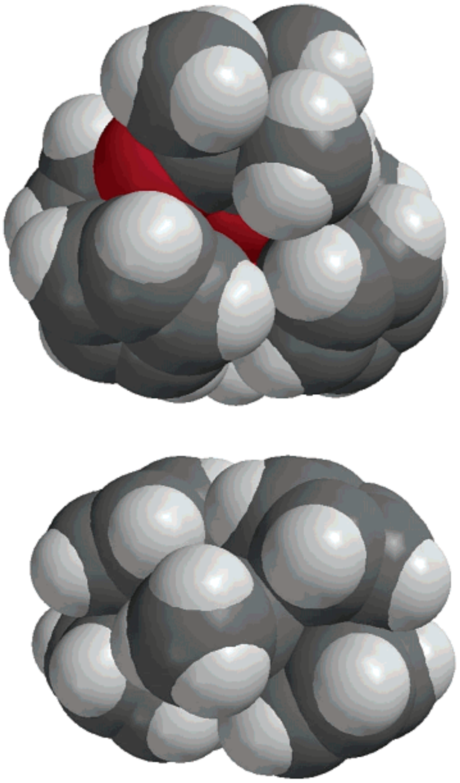

Figure 3. Space-filling diagrams of the dication of **3**.

---

(15) Attempts to avoid the formation of $Cp_2Zr\{\eta^2\text{-}C({=}O)Me\}(\mu\text{-}Me)B(C_6F_5)_3$ by increasing the CO pressure were unsuccessful, because high CO pressure (>1 atm) inhibits VC uptake.

Table 2. Selected Bond Lengths (Å) and Angles (deg) for 3

C(1)−O(1)	1.252(5)	C(1)−C(2)	1.463(5)
C(1)−Zr(2)	2.195(4)	C(3)−O(2)	1.443(4)
C(3)−C(5)	1.507(6)	C(3)−C(7)	1.512(6)
C(3)−C(4)	1.539(7)	C(5)−C(6)	1.365(8)
C(7)−O(3)	1.239(5)	C(7)−C(8)	1.487(5)
O(1)−Zr(1)	2.181(3)	O(1)−Zr(2)	2.290(3)
O(2)−Zr(1)	2.271(3)	O(2)−Zr(2)	2.296(3)
O(3)−Zr(1)	2.239(3)	Zr(1)−C(100)[a]	2.219
Zr(1)−C(200)[a]	2.217	Zr(2)−C(300)[a]	2.216
Zr(3)−C(400)[a]	2.196		
O(1)−C(1)−C(2)	119.6(4)	O(1)−C(1)−Zr(2)	78.0(2)
C(2)−C(1)−Zr(2)	162.3(3)	O(2)−C(3)−C(5)	111.5(3)
O(2)−C(3)−C(7)	106.4(3)	C(5)−C(3)−C(7)	105.9(4)
O(2)−C(3)−C(4)	111.0(4)	C(5)−C(3)−C(4)	113.0(5)
C(7)−C(3)−C(4)	108.6(4)	C(6)−C(5)−C(3)	120.6(6)
O(3)−C(7)−C(8)	118.9(4)	O(3)−C(7)−C(3)	119.6(4)
C(8)−C(7)−C(3)	121.5(3)	C(1)−O(1)−Zr(1)	177.3(3)
C(1)−O(1)−Zr(2)	69.7(2)	Zr(1)−O(1)−Zr(2)	113.0(1)
C(3)−O(2)−Zr(1)	121.3(2)	C(3)−O(2)−Zr(2)	129.2(2)
Zr(1)−O(2)−Zr(2)	109.5(1)	C(7)−O(3)−Zr(1)	123.3(3)
C300−Zr(2)−C400	127.8		

[a] C100 is the centroid of the C(9)−C(13) Cp ring; C200 is the centroid of the C(14)−C(18) Cp ring; C300 is the centroid of the C(19)−(23) Cp ring; C400 is the centroid of the C(24)−(28) Cp ring.

Zr(1) in a bidentate fashion. The Zr(1)−O(3) bond distance (2.239(3) Å) is slightly longer than those of typical Zr(IV) ketone complexes. The Zr(1)−O(2) (2.271(3) Å) and Zr(2)−O(2) (2.296(3) Å) distances are longer than of those in typical terminal or bridging Zr alkoxide complexes, such as $Cp_2Zr(O^tBu)\{Ru(CO)_2Cp\}$ (1.910 Å)[18] and $\{Cp^*(MeO)_2Zr(\mu\text{-}OMe)\}_2$ (μ-OMe: 2.176 Å).[19] The long Zr−O distances reflect the high Zr coordination number. The ring formed by Zr(1), O(2), C(3), C(7), and O(3) is slightly puckered such that C(3) deviates from the Zr(1)−O(2)−C(7)−O(3) plane by 0.089 Å. Several related O-chelated keto alkoxide complexes have been structurally characterized,[20−24] of which $(\eta^5\text{-}C_5H_4Me)_2Zr(Me)\{\kappa^2\text{-}OCH(p\text{-tol})C({=}O)Fe(CO)_4\}Li(THF)_2$[24] is most closely analogous to **3**. However, in this case the Zr-alkoxide unit is terminal rather than bridging, so the Zr−O(alkoxide) distance (2.13(1) Å) is shorter than that in **3**.

NMR Analysis of 3. Dissolution of **3** in THF-d_8 results in dissociation of the dinuclear dication into a 1:1 mixture of the solvated species $[Cp_2Zr\{\eta^2\text{-}C({=}O)Me\}(THF\text{-}d_8)][MeB(C_6F_5)_3]$ (**4**-d_8) and $[Cp_2Zr\{\kappa^2\text{-}OCMe(CH{=}CH_2)C({=}O)Me\}(THF\text{-}d_8)][MeB(C_6F_5)_3]$ (**5**-d_8), as shown in eq 4. Dissolution of **3** in THF followed by removal of the volatiles and redissolution in CD_2Cl_2 yields a 1:1 mixture of **4** and **5**. The NMR data for **4** agree with those of the corresponding BPh_4^- salt, which we prepared previously.[6b] The resonances for the coordinated THF (δ 4.18 (m), 2.14 (m)) are shifted from those of free THF in CD_2Cl_2 (δ 3.68 (m), 1.82 (m)). The ^1H NMR spectrum of **5** contains resonances for coordinated THF (δ 4.18 (m), 2.14 (m)) and the pendant vinyl group (δ 5.99 (dd, J = 17, 11), 5.44 (dd, J = 17, 1), and 5.39 (dd, J = 11, 1)). Two Cp resonances are expected for **5**, but only one is observed in the ^1H NMR spectrum (δ 6.23). However, the Cp and Zr-THF ^{13}C NMR resonances of **5** are broad. These observations suggest that **5** undergoes the exchange shown in eq 5, probably via chelate ring opening, THF exchange with site epimerization at Zr, and chelate ring closing. The coordination of the carbonyl oxygen to Zr of **5** is established by the low-field carbonyl ^{13}C NMR resonance at δ 230.6, which shifted downfield from the free ketone region (δ 206−218).[25] In addition, the IR spectrum of **5** displays a carbonyl absorption at $\nu_{CO} = 1505\ cm^{-1}$, which is typical of a ketone unit coordinated to a Lewis acid.[24]

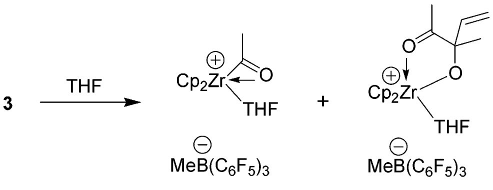

4 **5** (4)

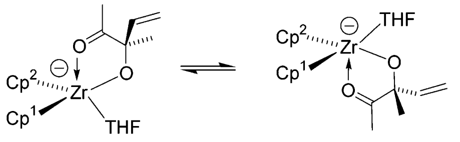

(5)

Reaction Mechanism. A reasonable mechanism for the formation of **3** is provided in Scheme 1. VC reacts with **1a**/**b** to form the VC adduct $Cp_2Zr\{\eta^2\text{-}C({=}O)Me\}(VC)^+$ (**6**), which undergoes 1,2 insertion to form $Cp_2Zr\{CH_2CHClC({=}O)CH_3\}^+$ (**7**). Intermediate **7** undergoes β-Cl elimination to yield MVK and Cp_2ZrCl^+ (**8**). The MVK is trapped by a second equivalent of **1a**/**b** to form the O-bound MVK adduct $Cp_2Zr\{\eta^2\text{-}C({=}O)Me\}(MVK)^+$ (**9**), which in turn undergoes 1,2 addition of the Zr-acyl group to the C═O bond of MVK to yield $Cp_2Zr\{\kappa^2\text{-}OC(Me)(CH{=}CH_2)C({=}O)Me\}^+$ (**10**). Intermediate **10** is ultimately trapped by a third equivalent of **1a**/**b** by bridging of the alkoxide and acyl ligands to form the final product **3**. The detailed fate of **8** is unknown, but we have shown previously that $[(C_5R_5)_2ZrCl][MeB(C_6F_5)_3]$ species readily decompose by ligand redistribution reactions.[2a] We believe that Cp_2ZrCl_2 and other Cp_2Zr species indicated in Scheme 1 are derived from **8**.

Confirmation of the Role of MVK. To confirm the proposed intermediacy of MVK in Scheme 1, the reaction of **1a**/**b** with MVK was studied (Scheme 2). The reaction of **1a**/**b** with 1 equiv of MVK in CD_2Cl_2 at −78 °C quantitatively yields MVK adduct **9**, which was characterized by ^1H and ^{13}C NMR spectroscopy at −75

---

(16) Galeffi, B.; Simard, M.; Wuest, J. D. *Inorg. Chem.* **1990**, *29*, 951.
(17) Sun, Y.; Piers, W. E.; Yap, G. P. A. *Organometallics* **1997**, *16*, 2509.
(18) Casey, C. P.; Jordan, R. F.; Rheingold, A. L. *J. Am. Chem. Soc.* **1983**, *105*, 665.
(19) Heyn, R. H.; Stephan, D. W. *Inorg. Chem.* **1995**, *34*, 2804.
(20) Wistuba, T.; Limberg, C.; Kircher, P. *Angew. Chem., Int. Ed.* **1999**, *38*, 3037.
(21) (a) Mialane, P.; Anxolabehere-Mallart, E.; Blondin, G.; Nivorojkine, A.; Guilhem, J.; Tchertanova, L.; Cesario, M.; Ravi, N.; Bominaar, E.; Girerd, J.-J.; Munck, E. *Inorg. Chim. Acta* **1997**, *263*, 367. (b) Attia, A. S.; Jung, O. S. Pierpont, C. G. *Inorg. Chim. Acta* **1994**, *226*, 91.
(22) Dutta, S.; Peng, S.-M.; Bhattacharya, S. *Inorg. Chem.* **2000**, *39*, 2231.
(23) Barbaro, P.; Bianchini, C.; Mealli, C.; Meli, A. *J. Am. Chem. Soc.* **1991**, *113*, 3181.
(24) Askham, F. R.; Carroll, K. M.; Briggs, P. M.; Rheingold, A. L.; Haggerty, B. S. *Organometallics* **1994**, *13*, 2139.
(25) Breitmaier, E.; Voelter, W. *Carbon-13 NMR Spectroscopy. High-Resolution Methods and Applications in Organic Chemistry and Biochemistry*, 3rd ed.; VCH Verlagsgesellschaft: Weinheim, Fed. Rep. Ger., 1987.

Scheme 1

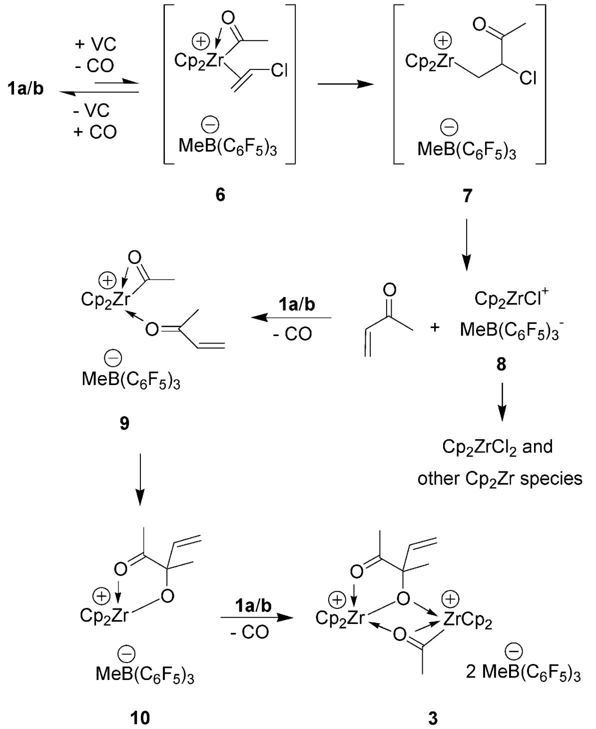

Scheme 2

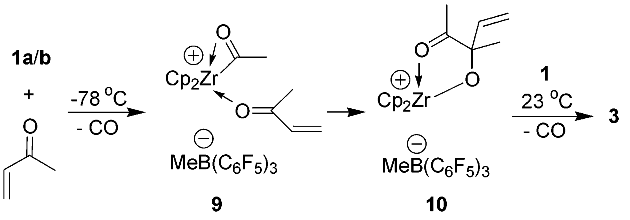

°C. The ^{13}C carbonyl resonance for the coordinated MVK in **9** is shifted downfield to δ 216.9, versus δ 199.6 for free MVK, while the MVK vinyl resonances are not significantly perturbed from the free MVK positions. These results indicate that the MVK in **9** coordinates through the oxygen. This result is consistent with the general trend for α,β-unsaturated carbonyl compounds to form σ-complexes with electron-deficient/poor-back-bonding metals,[26] rather than η^2-olefin π-complexes as observed for electron-rich metals.[27]

When **9** is warmed to 23 °C overnight, it converts to the chelated insertion product **10** (ca. 95% NMR yield). The ^{1}H NMR spectrum of **10** in CD_2Cl_2 is complex, possibly due to oligomerization. However, the ^{1}H NMR spectrum of **10** in THF-d_8 is identical to that of **5**-d_8 produced by dissolution of **3** in THF-d_8 (eq 4).

Regiochemistry of VC Insertion of Metal Acyl Complexes. The key result from these studies is that $Cp_2Zr\{\eta^2\text{-}C(=O)Me\}^+$ reacts with VC by 1,2 insertion (i.e., **6** → **7** in Scheme 1). This regioselectivity contrasts with the 2,1 VC insertion observed for $L_2Pd\{C(=O)Me\}^+$ cations (L_2 = R_2bipy, dppp, dmpe) in our previous studies.[4,5] We proposed earlier that 2,1 VC insertion is favored for $L_2Pd\{C(=O)Me\}^+$ species because the alternative 1,2 insertion product $L_2Pd\{CH_2CHClC(=O)Me\}^+$ would be destabilized by the presence of the electron-withdrawing Cl and acyl substituents on the β-carbon. Other factors that may contribute to the preference for 2,1 insertion include olefin distortion energies and steric interactions between the migrating acyl group and the VC Cl substituent.[28,29] This trend appears to be general as $L_2Pd\{C(=O)Me\}^+$ species containing a variety of ancillary ligands (L_2 = $Ph_2PNHC(O)Me$,[30] $(OC)_4Fe(\mu\text{-dppx})$,[31] *o*-(diphenylphosphino)-*N*-benzaldimine,[32] 1,10-phenanthroline,[33] 1,2-bis(diphenylphosphino)ethane,[34] and dppp[35]) undergo 2,1 insertion with other olefins that bear electron-withdrawing groups, such as acrylates, vinyl acetate, and methyl vinyl ketone. These results suggest that, in the $Cp_2Zr\{C(=O)Me\}^+$ case, the electronic preference for 2,1 VC insertion is overridden by steric factors. As illustrated in Scheme 3, steric crowding between the Cl and Cp groups disfavors the VC adduct, insertion product, and presumably the transition state for 2,1 insertion. Similarly, Busico's studies of the reaction of L_nZrCl_2/MAO (L_n = *rac*-dimethylsilylbis(2-methyl-4-phenyl-1-indenyl)) with propylene/CO showed that $L_nZr\{C(=O)R\}^+$ species undergo 1,2 propylene insertion.[7]

Conclusions

VC reacts with $Cp_2Zr\{\eta^2\text{-}C(=O)Me\}^+$ by 1,2 insertion, followed by β-Cl elimination, to form Cp_2ZrCl^+ and MVK. The MVK is trapped by 2 equiv of $Cp_2Zr\{\eta^2\text{-}C(=O)Me\}^+$ to yield the unusual dinuclear dicationic μ-acyl

---

(26) (a) Shambayati, S.; Crowe, W. E.; Schreiber, S. L. *Angew. Chem., Int. Ed. Engl.* **1990**, *29*, 256. (b) Shambayati, S.; Schreiber, S. L. In *Comprehensive Organic Synthesis*; Trost, B. M., Fleming, I., Eds.; Pergamon: Oxford, U.K., 1991; Vol. 1; p 283. (c) Poll, T.; Metter, J. O.; Helmchen, G. *Angew. Chem., Int. Ed. Engl.* **1985**, *24*, 112. (d) Lewis, F. D.; Oxman, J. D.; Huffman, J. C. *J. Am. Chem. Soc.* **1984**, *106*, 466. (e) Honeychuck, R. V.; Bonnesen, P. V.; Farahi, J.; Hersh, W. H. *J. Org. Chem.* **1987**, *52*, 5293.

(27) (a) Motoyama, Y.; Kurihara, O.; Murata, K.; Aoki, K.; Nishiyama, H. *Organometallics* **2000**, *19*, 1025. (b) Motoyama, Y.; Murata, K.; Kurihara, O.; Naitoh, T.; Aoki, K.; Nishiyama, H. *Organometallics* **1998**, *17*, 1251 (c) Kegley, S. E.; Walter, K. A.; Bergstrom, D. T.; MacFarland, D. K.; Young, B. G.; Rheingold, A. L. *Organometallics* **1993**, *12*, 2339. (d) Ferrara, M. L.; Orabona, I.; Ruffo, F.; Funicello, M.; Panunzi, A. *Organometallics* **1998**, *17*, 3832. (e) Selvakumar, K.; Valentini, M.; Wörle, M.; Pregosin, P. S.; Albinati, A. *Organometallics* **1999**, *18*, 1207. (f) Castarlenas, R.; Esteruelas, M. A.; Martin, M.; Oro, L. A. *J. Organomet. Chem.* **1998**, *564*, 241. (g) Yi, C. S.; Torres-Lubian, J. R.; Liu, N.; Rheingold, A. L.; Guzei, I. A. *Organometallics* **1998**, *17*, 1257. (h) Jedlicka, B.; Rülke, R. E.; Weissensteiner, W.; Fernández-Galán, R.; Jalón, F. A.; Manzano, B. R.; Rodríguez-de la Fuente, J.; Veldman, N.; Kooijman, H.; Spek, A. L. *J. Organomet. Chem.* **1996**, *516*, 97. (i) Miller, K. J.; Kitagawa, T. T.; Abu-Omar, M. M. *Organometallics* **2001**, *20*, 4403. (j) Ganguly, S.; Roundhill, D. M. *Organometallics* **1993**, *12*, 4825. (k) Bennett, M. A.; Jin, H.; Li, S.; Rendina, L. M.; Willis, A. C. *J. Am. Chem. Soc.* **1995**, *117*, 8335.

(28) (a) Michalak, A.; Ziegler, T. *J. Am. Chem. Soc.* **2001**, *123*, 12266. (b) Michalak, A.; Ziegler, T. *Organometallics* **1999**, *18*, 3998. (c) von Schenck, H.; Strömberg, S.; Zetterberg, K.; Ludwig, M.; Åkermark, B.; Svensson, M. *Organometallics* **2001**, *20*, 2813.

(29) For DFT studies of insertion reactions of Pd-acyl species see: (a) Margl, P.; Ziegler, T. *J. Am. Chem. Soc.* **1996**, *118*, 7337. (b) Margl, P.; Zielger, T. *Organometallics* **1996**, *15*, 5519. (c) Cavallo, L. *J. Am. Chem. Soc.* **1999**, *121*, 4238.

(30) Braunstein, P.; Frison, C.; Morise, X. *Angew. Chem., Int. Ed.* **2000**, *39*, 2867.

(31) dppx = $Ph_2PNHPPh_2$. Braunstein, P.; Durand, J.; Knorr, M.; Strohmann, C. *J. Chem. Soc., Chem. Commun.* **2001**, 211.

(32) (a) Reddy, K. R.; Surekha, K.; Lee, G. H.; Peng, S. M.; Chen, J. T.; Liu, S. T. *Organometallics* **2001**, *20*, 1292. (b) Reddy, K. R.; Chen, C. L.; Liu, Y. H.; Peng, S. M.; Chen, J. T.; Liu, S. T. *Organometallics* **1999**, *18*, 2574.

(33) Rix, F. C.; Brookhart, M.; White, P. S. *J. Am. Chem. Soc.* **1996**, *118*, 4746.

(34) Ozawa, F.; Hayashi, T.; Koide, H.; Yamamoto, A. *J. Chem. Soc., Chem. Commun.* **1991**, 1469.

(35) Dekker, G. P. C. M.; Elsevier, C. J.; Vrieze, K.; van Leeuwen, P. W. N. M.; Roobeek, C. F. *J. Organomet. Chem.* **1992**, *430*, 357.

Scheme 3

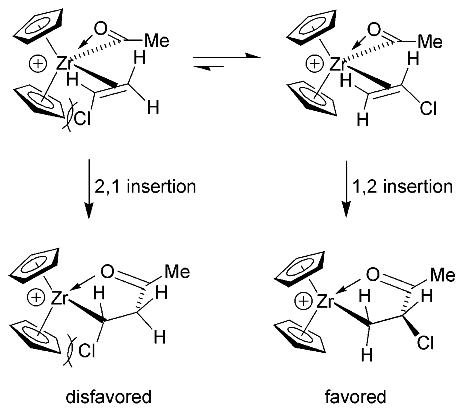

μ-(keto-alkoxide) complex **3**. The 1,2 VC insertion regiochemistry contrasts with the 2,1 regiochemistry observed for VC insertion of $L_2Pd\{C(=O)Me\}^+$ species and appears to be controlled by steric factors.

Experimental Section

General Procedures. All manipulations were performed using drybox or Schlenk techniques under an N_2 atmosphere or on a high-vacuum line unless otherwise indicated. Solvents were distilled from appropriate drying/deoxygenating agents (THF and THF-d_8: sodium benzophenone ketyl; CH_2Cl_2 and C_6H_5Cl: CaH_2; CD_2Cl_2 and C_6D_5Cl: P_4O_{10}). Pentane and benzene were purified by passage through columns of activated alumina and BASF R3-11 oxygen removal catalyst. Nitrogen was purified by passage through columns containing activated molecular sieves and Q-5 oxygen scavenger. CO was purchased from Matheson. $B(C_6F_5)_3$ was supplied by Boulder Scientific. Cp_2ZrMe_2 was synthesized according to the literature procedure.[36] VC and all other chemicals were purchased from Aldrich and used without further purification, except for MVK, which was dried by 3 Å molecular sieves and stored under vacuum at −20 °C. VC and MVK were quantified by use of a calibrated gas bulb. Elemental analyses were performed by Midwest Microlab.

NMR spectra were recorded on Bruker DMX-500 or DRX-400 spectrometers, in Teflon-valved tubes, at 23 °C unless otherwise indicated. ^{1}H and ^{13}C chemical shifts are reported versus $SiMe_4$ and were determined by reference to residual ^{1}H and ^{13}C solvent signals. ^{11}B chemical shifts are referenced to external $Et_2O \cdot BF_3$. ^{19}F chemical shifts are reported relative to $CFCl_3$. All coupling constants are reported in Hz. Nuclear Overhauser effect spectroscopy (NOESY), ^{1}H−^{1}H correlation spectroscopy (COSY), DEPT (distortionless enhancement by polarization transfer), and heteronuclear multiple quantum correlation spectroscopy (HMQC) spectra were acquired and processed using standard Bruker programs.

NMR spectra for cationic complexes contain resonances for the free $MeB(C_6F_5)_3^-$. ^{1}H NMR (CD_2Cl_2, −75 °C): δ 0.34 (br s, *Me*B). ^{13}C NMR (CD_2Cl_2, −75 °C): δ 147.4 (dd, J = 236, 10, C_6F_5), 136.9 (d, J = 242, C_6F_5), 135.9 (dd, J = 236, 10, C_6F_5), 127.6 (br s, *ipso*-C_6F_5), 9.22 (br s, *Me*B). ^{11}B NMR (CD_2Cl_2, −75 °C): δ −14 (br s). ^{19}F NMR (CD_2Cl_2, −75 °C): δ −134.6 (br s, 8F, F_{ortho}), −168.7 (t, J = 21, 4F, F_{para}), −170.9 (t, J = 17, 8F, F_{meta}).

Data for Free MVK. ^{1}H NMR (CD_2Cl_2): δ 6.28 (dd, J = 18, 10, 1H), 6.15 (dd, J = 18, 1, 1H), 5.88 (dd, J = 10, 1, 1H), 2.24 (s, 3H). ^{13}C NMR (CD_2Cl_2): δ 198.9, 137.8, 129.0, 26.5. ^{1}H NMR (CD_2Cl_2, −75 °C): δ 6.19 (m, 2H, coincidental vinyl H), 5.96 (dd, J = 6.5, 5.0, 1H), 2.23 (s, 3H). ^{13}C NMR (CD_2Cl_2): δ 199.6, 136.9, 130.1, 25.9.

[$Cp_2Zr\{\eta^2$-C(=O)Me}(CO)][$MeB(C_6F_5)_3$] (O-inside/O-outside: 1a/1b). A CD_2Cl_2 solution of this compound was prepared in a valved NMR tube by carbonylation of Cp_2ZrMe-(μ-Me)$B(C_6F_5)_3$ as described previously.[5] The isomer ratio **1a**/**b** is 5:1 at 23 °C and 2.7:1 at −75 °C. ^{1}H NMR (CD_2Cl_2, −75 °C): δ 6.09 (s, 2.7H, Cp **1a**), 5.99 (s, 7.3H, Cp **1b**), 3.17 (s, 2.2H, C(=O)*Me* **1a**), 3.15 (s, 0.8H, C(=O)*Me* **1b**), 0.40 (br s, 3H). ^{13}C{^{1}H} NMR (CD_2Cl_2, −75 °C): δ 305.2, 297.1, 198.0, 191.8, 109.1, 107.8, 34.0, 33.1.

Synthesis of 3 by Reaction of 1 with VC. A valved NMR tube containing a clear solution of **1a/b** (0.0398 mmol) in CD_2Cl_2 (0.5 mL) was frozen, evacuated under vacuum, and charged with VC (0.557 mmol) at − 196 °C. The tube was warmed to 23 °C and briefly shaken. A yellow crystalline solid formed within 1 h. The tube was maintained at 23 °C overnight. The supernatant was decanted under N_2. The crystalline solid was washed with fresh CH_2Cl_2 (3 × 0.5 mL) and dried under vacuum to afford **3** as a yellow solid (18.2 mg, 79%). The solid was dissolved in THF-d_8 and analyzed by NMR, which showed that a 1.08:1 mixture of [$Cp_2Zr\{\eta^2$-C(=O)Me}(THF-d_8)$^+$][$MeB(C_6F_5)_3$] (**4**-d_8) and [$Cp_2Zr\{\kappa^2$-OCMe(CH=CH_2)C(=O)Me}(THF-d_8)][$MeB(C_6F_5)_3$] (**5**-d_8) was present. NMR data for these species are given below.

Synthesis of 3 by Reaction of 1 with MVK. A valved NMR tube containing a solution of **1a/b** (0.0398 mmol) in CD_2Cl_2 (0.5 mL) was frozen, evacuated under vacuum, and charged with MVK (0.0199 mmol) at − 196 °C. The tube was warmed to 23 °C and briefly shaken. A yellow crystalline solid started to form within 1 h. The tube was maintained at 23 °C overnight. The pale yellow supernatant was decanted under N_2. The crystalline solid was washed with CH_2Cl_2 (3 × 0.5 mL) and dried under vacuum to afford a yellow solid (29.9 mg, 91%). Anal. Calcd for $C_{66}H_{38}B_2F_{30}O_3Zr$: C, 47.95; H, 2.32. Found: C, 47.61; H, 2.40. The ^{1}H and ^{13}C NMR spectra in THF-d_8 of this product matched those of **3** obtained from the reaction of **1** and VC and are consistent with the dissociation of **3** into a 1:1 mixture of [$Cp_2Zr\{\eta^2$-C(=O)Me}(THF-d_8)][$MeB(C_6F_5)_3$] (**4**-d_8) and [$Cp_2Zr\{\kappa^2$-OCMe(CH=CH_2)C(=O)Me}(THF-d_8)][$MeB(C_6F_5)_3$] (**5**-d_8). Data for **4**-d_8: ^{1}H NMR (THF-d_8): δ 6.12 (s, 10H), 3.19 (s, 3H). ^{13}C{^{1}H} NMR (THF-d_8): δ 318.8 (Zr{*C*(=O)Me}), 111.5 (Cp), 33.5 (Zr{C(=O)*Me*}). **5**-d_8: ^{1}H NMR (THF-d_8): δ 6.34 (s, 10H), 6.16 (dd, J = 17, 10, 1H), 5.50 (dd, J = 17, 1, 1H), 5.34 (dd, J = 10, 1, 1H), 2.52 (s, 3H), 1.52 (s, 3H). ^{13}C{^{1}H} NMR (THF-d_8): δ 231.5 (Zr−O=*C*), 138.2 (*C*H=CH_2), 117.1 (CH=*C*H_2), 116.3 (Cp), 98.1 (*tert-C*), 24.9 (*Me*), 24.7 (*Me*).

Reaction of 3 with THF. A sample of **3** prepared from **1a**/**b** and 0.5 equiv of MVK was dissolved in THF to form a clear, pale yellow solution. The volatiles were removed under vacuum, and CH_2Cl_2 (0.5 mL) was added to form a clear, pale yellow solution. The volatiles were removed under vacuum. The CH_2Cl_2 treatment was repeated four times to ensure complete removal of free THF. Finally CD_2Cl_2 (0.5 mL) was added by vacuum transfer. ^{1}H and ^{13}C NMR spectra were obtained, which established that a 1:1 mixture of [$Cp_2Zr\{\eta^2$-C(=O)Me}(THF)][$MeB(C_6F_5)_3$] (**4**) and [$Cp_2Zr\{\kappa^2$-OCMe(CH=CH_2)C(=O)Me}(THF)][$MeB(C_6F_5)_3$] (**5**) had formed; THF exchange between these species is slow on the NMR time scale at 23 °C in CD_2Cl_2 solution. Data for **4**: ^{1}H NMR (CD_2Cl_2): δ 5.98 (s, 10H), 4.00 (br m, Zr-*THF*), 3.13 (s, 3H), 2.05 (br m, 4H, Zr-*THF*). ^{13}C{^{1}H} NMR (CD_2Cl_2): δ 317.5 (Zr{*C*(=O)Me}), 110.5 (Cp), 76.7 (Zr-*THF*), 33.9 (Zr{C(=O)*Me*}), 25.9 (Zr-*THF*). Data for **5**: ^{1}H NMR (CD_2Cl_2): δ 6.23 (10H), 5.99 (dd, J = 17, 11, 1H), 5.44 (dd, J = 17, 1, 1H), 5.39 (dd, J = 11, 1, 1H), 4.18 (m, 4H, Zr-*THF*), 2.45 (s, 3H), 2.14 (m, 4H, Zr-*THF*), 1.48 (s, 3H). ^{13}C{^{1}H} NMR (CD_2Cl_2): δ 230.6 (Zr−O=*C*), 136.4 (*C*H=CH_2), 117.7 (CH=*C*H_2), 115.4 (Cp), 74.8 (br s, Zr-*THF*), 25.7 (br s, Zr-*THF*), 25.0 (*Me*), 24.8 (*Me*); *tert*-C resonance was not observed. These NMR assignments were confirmed by COSY, DEPT, and HMQC experiments.

---

[36] Samuel, E.; Rausch, M. D. *J. Am. Chem. Soc.* **1973**, *95*, 19.

Table 3. Summary of Crystallographic Data for Compounds 1a and 3

	1a	3
formula	$C_{32}H_{16}BF_{15}O_2Zr$	$C_{66}H_{38}B_2F_{30}O_3Zr_2$
fw	819.48	1653.02
cryst size (mm)	0.24 × 0.08 × 0.08	0.15 × 0.10 × 0.07
d(calc), Mg/m^3	1.806	1.818
cryst syst	monoclinic	triclinic
space group	$P2_1/c$	$P\bar{1}$
a, Å	12.676(2)	12.508(3)
b, Å	16.046(2)	12.831(3)
c, Å	15.604(2)	21.375(5)
α, deg		94.578(4)
β, deg	108.280(3)	92.907(3)
γ, deg		117.425(3)
V, Å^3	3013.7(8)	3020(1)
Z	4	2
T (K)	100	100
diffractometer	Bruker SMART APEX	Bruker SMART APEX
radiation, λ (Å)	Mo Kα, 0.71073	Mo Kα, 0.71073
2θ range (deg)	2.12−25.03	2.13−28.32
index ranges: h; k; l	−14, 15; −15, 19; −16, 18	−16, 16; −17, 17; −18, 18
no. of reflns collected	15 102	35 480
no. of unique reflns	5325	14 114
no. of obsd reflns	$I > 2\sigma(I)$, 5119	$I > 2\sigma(I)$, 12 569
R_{int}	0.0284	0.0326
μ, mm^{-1}	0.490	0.489
max./min. transmn	1.0, 0.895	1.0, 0.777
structure solution	direct methods[a]	direct methods[a]
refinement method	full-matrix least squares on F^2	full-matrix least squares on F^2
no. of data/restraints/params	5325/0/463	14114/0/933
adsorp corr	SADABS based on redundant diffractions	SADABS based on redundant diffractions
GOF on F^2	1.239	1.090
R indices ($I > 2\sigma(I)$)[b]	R1 = 0.0506, wR2 = 0.0985	R1 = 0.0611, wR2 = 0.1497
R indices (all data)[b]	R1 = 0.0536, wR2 = 0.0997	R1 = 0.0685, wR2 = 0.1552
max. diff peak/hole (e/Å^3)	0.460, −0.706	3.809, −1.318

[a] *SHELXTL-Version* 5.1; Bruker Analytical X-ray Systems: Madison, WI. [b] $R1 = \sum||F_o| - |F_c||/\sum|F_o|$ and $wR2 = [\sum[w(F_o^2 - F_c^2)^2]/\sum[w(F_o^2)^2]]^{1/2}$, where $w = q/[\sigma^2(F_o^2) + (aP)^2 + bP]$.

Generation of [Cp$_2$Zr{η^2-C(=O)Me}(MVK)][MeB(C$_6$F$_5$)$_3$] (9). A solution of **1a/b** (0.0398 mmol) in CD_2Cl_2 (0.5 mL) was charged with MVK (0.0398 mmol) at − 196 °C. The mixture was warmed to −78 °C. A ^{1}H NMR spectrum was obtained and established that **9** had formed quantitatively. Two Cp resonances were observed in the ^{1}H and ^{13}C NMR spectra which is ascribed to the presence of two isomers, probably O-inside and O-outside isomers. ^{1}H NMR (CD_2Cl_2, −75 °C): δ 6.78 (dd, J = 14, 3, 1H, vinyl), 6.59 (m, 2H, vinyl), 6.35 (s, 1H, Cp of minor isomer), 5.94 (s, 9H, Cp of major isomer), 3.06 (s, 3H), 2.65 (s, 3H). ^{13}C{^{1}H} NMR (CD_2Cl_2, −75 °C): δ 317.7, 216.9, 141.3, 135.1, 115.2 (Cp of minor isomer), 110.1 (Cp of major isomer), 34.0, 26.1.

Generation of [Cp$_2$Zr{κ^2-OCMe(CH=CH$_2$)C(=O)Me}][MeB(C$_6$F$_5$)$_3$] (10). A solution of **9** generated as described above was maintained at 23 °C overnight. The volatiles were removed under vacuum, and THF-d_8 was added by vacuum transfer. A ^{1}H NMR spectrum was obtained and showed that **5**-d_8 had formed in ca. 95% NMR yield. ^{1}H NMR (THF-d_8): δ 6.35 (s, 10H), 6.16 (dd, J = 17, 10, 1H), 5.50 (dd, J = 17, 1, 1H), 5.34 (dd, J = 10, 1, 1H), 2.51 (s, 3H), 1.52 (s, 3H).

X-ray Crystallographic Analysis of 1a and 3. Single crystals of **1a** were grown from CH_2Cl_2 at −80 °C. Single crystals of **3** were obtained from the reaction of **1a**/**b** with MVK in CD_2Cl_2 at 23 °C. Crystal data, data collection details, and solution and refinement procedures are summarized in Table 3, and full details are provided in the Supporting Information. The ORTEP diagrams were drawn with 50% probability ellipsoids. All non-hydrogen atoms were refined with anisotropic displacement coefficients. All hydrogen atoms were included in the structure factor calculation at idealized positions and were allowed to ride on the neighboring atoms with relative anisotropic displacement coefficients.

Acknowledgment. We thank Dr. Ian Steele for assistance with X-ray diffraction analyses. This work was supported by the Edison Polymer Innovation Corporation and the Department of Energy (DE-FG02-00ER15036).

Supporting Information Available: Text, figures, and tables that give crystallographic data for **1a** and **3**. This material is available free of charge via the Internet at http://pubs.acs.org.

OM0210311